ingegneria sismica
International Journal of Earthquake Engineering
Anno XXXV – Num. 3

DIRECTIONALITY MODELS FROM GROUND MOTIONS OF ITALY

Luis A. Pinzón[1], Luis G. Pujades[1], Diego A. Hidalgo-Leiva[2] and Sergio A. Díaz[3]

[1]Department of Civil and Environmental Engineering, Technical University of Catalonia, Barcelona, Spain

[2]Civil Engineering School, University of Costa Rica, San Jose, Costa Rica

[3]Academic Division of Engineering and Architecture, Universidad Juárez Autónoma de Tabasco, Tabasco, Mexico

SUMMARY: *Directionality effects on the expected strong ground motion in Italy are investigated. After a brief description of the directionality effect and the intensity measures involved, a wide Italian database[1] of strong ground motion records is used, with a total of 949 horizontal accelerograms (two components). The analysis is performed for 5% damped response spectra in the 0.01–4 s period range. Rotation-independent intensity measures, resulting from combining maximum values of the as-recorded accelerograms, are investigated. The study has also been performed using maximum values of the time histories resulting from the previous combination of as-recorded time histories. Ratios between these rotation-independent intensity measures and those formerly used in ground motion predictive equations have been computed and modelled by means of a simple theoretical model. Thus, the results are useful for updating former strong ground motion predictive equations in a simple and straightforward way.*

KEYWORDS: *directionality, seismic response, intensity measures, orientation-independent, spectral response*

1 Introduction

Most ground motion prediction equations (GMPE) use as intensity measures (IMs) the peak ground acceleration and the 5% damped spectral response of a single degree of freedom (SDOF) system corresponding to the as-recorded horizontal ground motions [Beyer and Bommer, 2006, Douglas, 2017]. Moreover, there are many ways to combine the peak values of these two as-recorded horizontal components in the GMPEs [Douglas, 2003]: the arithmetic mean (AM), the geometric mean (GM), or the largest value of both components (Largest) are three of them. The GM of the response spectra is the most commonly used IM. An advantage of the GM is that the variability of the results of regressions used in the GMPEs is lower than with other measures [Beyer and Bommer, 2006]. However, the GM of the response spectra have a potentially significant drawback: they are not invariant to sensor orientation. Therefore, these measures differ for the same soil strong motion depending on the orientation of the recording instrument.

[1] Italian Accelerometric Archive (ITACA): http://itaca.mi.ingv.it/ItacaNet/ (last accessed 26 May 2017)

Corresponding author: Luis A. Pinzón, Department of Civil and Environmental Engineering, Technical University of Catalonia, Spain.
Email: luis.pinzon@upc.edu

As an extreme case, let us consider a noise-free, polarized signal. If one of the sensors is aligned with the direction of polarization, the GM of the response spectra of the as-recorded ground motion would be zero. This is an essential consideration for near-fault records. In these cases, the rupture orientation and the radiation pattern, including directivity effects, can produce strong motions correlated for 1 s or for longer periods [Spudich *et al.*, 2004]. The directionality effects are present, more or less significantly, in any pair of strong ground motion records [Pinzón *et al*., 2018].

For these reasons, various sensor orientation-independent measures have been proposed, including: GMRotDpp, GMRotIpp, RotDpp, and RotIpp [Boore *et al*., 2006, Boore, 2010]. In these measures "GM" means geometric mean, "Rot" means rotation, letters D and I indicate dependent and independent of the period, and "pp" represents the percentile. Generally, the 50th percentile is used in GMPEs. By using these new measures, the sensor orientation effect is eliminated as a component of epistemic uncertainty. This correction may be important in assessments of the probabilistic seismic risk due to ground motions with long return periods [Bommer *et al*., 2004]. Moreover, in determinations of IMs, the maximum values of two time histories are usually combined, thus mixing up peak values that normally occur at different time instants, leading to meaningless and biased results.

The main purpose of this study is to assess ground-motion directionality effects in Italy. To this end, the Italian Accelerometric Archive (ITACA) will be used. Another goal is to propose new sensor orientation-independent IMs, which are based on the maximum values of the time history obtained by combining the two horizontal components, rather than on the combination of the two maximum values of each component. These new IMs will be called LRotDpp for the Larger measure, and mpGM, mpGMRotDpp, and mpGMRotIpp for the IMs involving geometric mean values as defined above. Finally, to provide adequate corrections for former IMs, which were obtained without considering directionality effects, IM ratios will be obtained and modelled. These ratios will allow us to update previous GMPEs in an easy and straightforward way.

However, because of the number and involvedness of the IMs in this study, first a specific section is devoted to clearly describing these quantities and explaining how they are computed for a single time histories pair.

2 Time histories

In this section, the main ways of considering time histories in directionality analyses are summarized and briefly described.

2.1 As-recorded time histories

Usually, accelerometric stations are equipped with three orthogonal sensors, EW, NS and Z. Generally, only the two horizontal components are used in probabilistic seismic hazard analysis (PSHA), seismic design, and seismic risk assessment. These time histories can come also from instrumented buildings or civil facilities such as bridges or nuclear power plants. In these cases, the orientation of the sensors is often linked to the geometry of the instrumented structure, and transversal and longitudinal sensors are frequently used. Two horizontal accelerograms, EW and NS components, recorded at the station T1213 are used as examples of acceleration time histories. The records correspond to the Central Italy, Mw=6.5, Umbria earthquake, which occurred on 30 October 2016 at 06:40:18 [INGV, 2016]. Data have been

downloaded from the ITACA strong motion database and are provided with the baseline removed [Paolucci *et al*., 2011, Pacor *et al*., 2011]. These EW and NS as-recorded time histories and their amplitude Fourier spectra are shown in Figure 1.

2.2 Response time histories

Many seismic design and seismic risk assessment methodologies are based on the response of single degree of freedom (SDOF) systems. Maximum values of the responses lead to response spectra. The equation of motion of an SDOF system, with a mass *m*, moving on a frictionless surface, driven by horizontal ground motion with acceleration $\ddot{U}(t)$, with a spring with stiffness *k*, and a dashpot with a coefficient of viscous damping *c* is [Douglas 2003, Chopra 2017]:

$$\ddot{u}(t) + 2\xi\omega\dot{u}(t) + \omega^2 u(t) = -\ddot{U}(t) \tag{1}$$

In this equation, ξ is the fraction of critical damping of the system, $\xi = c/(2\omega m)$, and T is the period of the SDOF vibrating system, $T = 2\pi\sqrt{m/k} = 2\pi/\omega$. $acc(t) = \ddot{u}(t) + \ddot{U}(t)$ is the absolute acceleration response, $\ddot{u}(t)$, $\dot{u}(t)$ and $u(t)$ are the relative acceleration, velocity and displacement responses, respectively. Typical ξ values for buildings are in the range of 0.05 to 0.2 and typical periods are in the range of 0.1 to 10 s. Because different periods and damping values are involved in seismic design and in damage and risk assessments, $\ddot{u}(t)$ and, therefore, $acc(t)$, $\dot{u}(t)$, and $u(t)$ really depend on the damping ratio, ξ, and the period, T. Maximum values of these responses define the well-known acceleration, velocity, and displacement response spectra; that is:

$$\begin{aligned} Sa(T,\xi) &= \max(|\ddot{u}(t,T,\xi) + \dot{u}(t)|)_{for\ t} = \max(|acc(t,T,\xi|)_{for\ t} \\ Sv(T,\xi) &= \max(|\dot{u}(t,T,\xi)|)_{for\ t} \\ Sd(T,\xi) &= \max(|u(t,T,\xi)|)_{for\ t} \end{aligned} \tag{2}$$

For $T = 0$, these values are known as peak ground acceleration (PGA), peak ground velocity (PGV), and peak ground displacement (PGD). PGA, PGV and PGD are ξ-independent.

The 5% damped acceleration response spectra have been computed for the accelerograms shown in Figure 1. In addition, the acceleration responses of an SDOF system with $\xi = 0.05$, 5% of critical damping, and T=0.17 s, have also been computed. The 0.17 period has been chosen because, as it will be seen below (see Figure 1), the maximum spectral responses in the two as recorded accelerograms are obtained close to this period. The Nigam and Jennings method [1969] has been used to compute responses and response spectra. For this case study, Figure 1 also displays the acceleration response time histories for a 5% damped SDOF system with a period T=0.17 s. The 5% damped acceleration response spectra are also shown. The 0.17 s period is marked in the amplitude Fourier spectra and in the response spectra. Peak values are also marked in the corresponding time histories. Table 1 shows these peak values and the time instants at which they are attained.

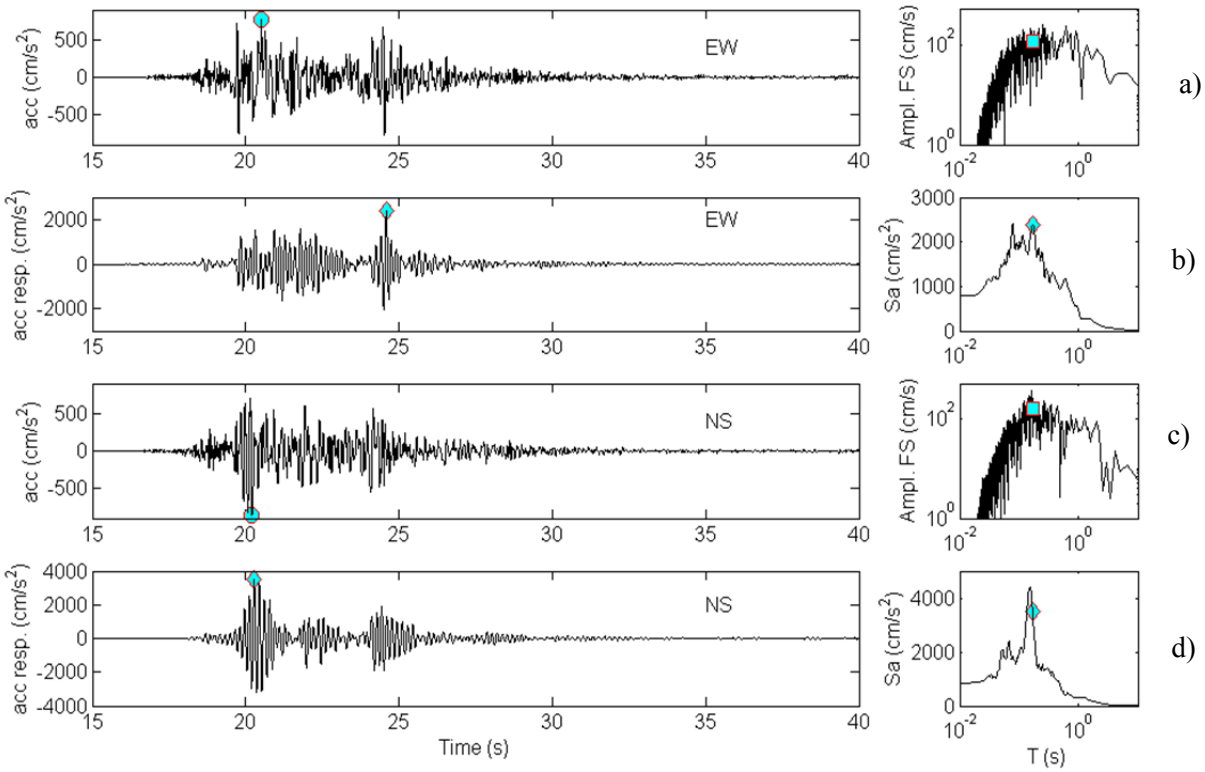

Figure 1. *As-recorded EW (a) and NS (c) accelerograms in the time and frequency domains. 5% damped acceleration responses for T=0.17 and 5% damped acceleration response spectra, Sa (T), for the EW (b) and NS (d) registers. The 0.17 s period is marked in the Fourier and response spectra, and maximum values are marked in the time histories.*

Table 1. *Maximum values and times at which they are attained for the EW and NS as-recorded accelerograms and acceleration responses of a 5% damped SDOF system with a period of 0.17 s. (See Figure 1).*

Period	EW as-recorded component		NS as-recoded component	
	Max (cm/s^2)	t_{max} (s)	Max (cm/s^2)	t_{max} (s)
T=0.00 s	760	20.51	-850	20.21
T=0.17 s	2254	24.58	3452	20.27

3 Directionality analysis

In engineering seismology and earthquake engineering, GMPE and design specifications have been based on maximum or peak values of as-recorded strong motion. The point is how the two peak values, coming from two orthogonal accelerograms, are obtained and, mainly, how they are combined in a rational way.

Clearly, strong dependence on the azimuth of the recording sensors is expected, and it is convenient to define rotation-independent measures. In this section these issues are tackled. The most common ways of quantifying peak values and response spectra are described and new ways of dealing with peak values with more physical sense are investigated.

3.1 Rotated (Rot) time histories

It is well-known that as-recoded time histories strongly depend on the orientation of the sensor. This may be critical for polarized strong motions. Rotated time histories corresponding to the combination of two as-recorded time histories are the time histories that would have been recorded by seismic sensors rotated by an angle, θ. Rotated time histories, $acc_1(t,\theta,T,\xi)$ and $acc_2(t,\theta,T,\xi)$, of the acceleration responses $acc_1(t,0,T,\xi)$ and $acc_2(t,0,T,\xi)$ of the as-recorded time histories are obtained according to the following equations:

$$\begin{aligned} acc_1(t,\theta,T,\xi) &= acc_1(t,0,T,\xi)\cos\theta + acc_2(t,0,T,\xi)\sin(\theta) \\ acc_2(t,\theta,T,\xi) &= -acc_1(t,0,T,\xi)\sin\theta + acc_2(t,0,T,\xi)\cos(\theta) \end{aligned} \quad (3)$$

Usually, $acc_1(t,0,0,0)$ and $acc_2(t,0,0,0)$ are the as-recorded EW and NS accelerograms. Rot-time-histories of responses may be obtained in the same way. In some cases, it may be useful to analyze only one of the two Rot orthogonal time histories, that is $acc_1(t,0,T,\xi)$ or $acc_2(t,0,T,\xi)$. For reasons of symmetry, in these cases, θ-angles are considered in the range between 0 and 180º. When the two components are analyzed, the angle range between 0 and 90º is sufficient.

3.2 Peak values and IMs

To see how maximum values vary with the orientation of the recording accelerographs, Figure 2a shows the peak values, PGAs, and the time instants at which they are achieved as functions of the angle, θ. Figure 2b shows the maximum values (Sa) of the responses of a 5% damped SDOF system with period T=0.17 s. Maximum values of the two orthogonal components are attained at different time instants. Differences in the order of 5 s may occur in this case.

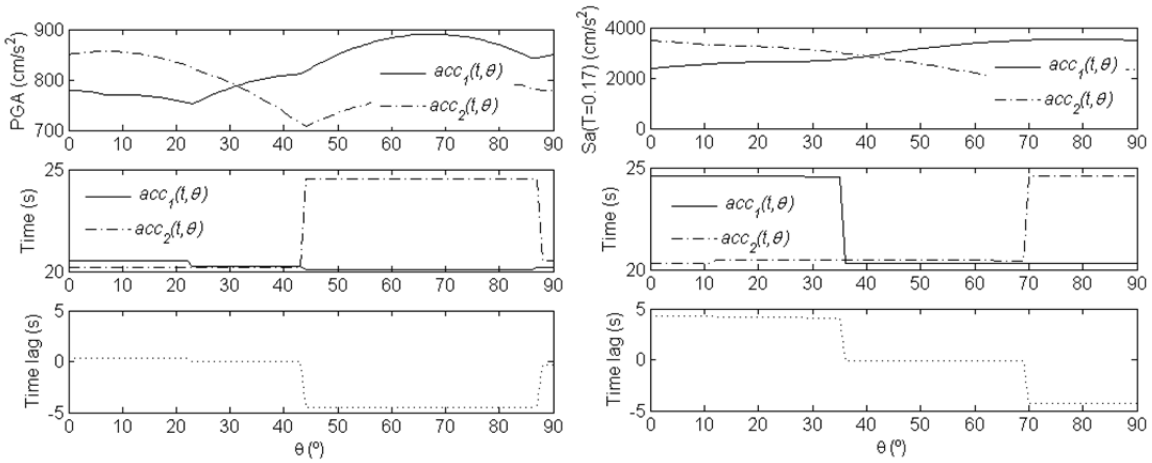

Figure 2. *a) Maximum values of the rotated accelerograms; the corresponding time arrivals (middle) and time lags (down) are also depicted. b) Same as a) for the responses of the rotated accelerograms for a 5% damped SDOF system with T=0.17 s. See also Figure 1*

There are several ways of combining peak values to obtain two-component-based intensity measures. The main IMs involved in the assessment of seismic directionality effects are described in this section. The geometric mean (GM) and the vector composition (VC) of the maximum values are discussed below. Let us call GM and VC these two quantities. Note that, often these IMs could not be attained in real cases, because the maximum quantities involved are not concurrent, so their physical meaning is poor. However, it is also true that statistically average or median values of GM and VC may be adequate for representing expected IMs. In this study, an alternative way of obtaining maximum values is also considered. The idea is to combine the time histories and then determine the maximum values of the resulting time histories. This way, maximum values would correspond to a specific time instant. The following equations are used for *pGM* and *pVC* combinations:

$$\begin{aligned} pGM(t,\theta,T,\xi) &= \left| acc_1(t,\theta,T,\xi)\ acc_2(t,\theta,T,\xi) \right|^{1/2} \\ pVC(t,\theta,T,\xi) &= \left[acc_1^2(t,\theta,T,\xi) + acc_2^2(t,\theta,T,\xi) \right]^{1/2} \end{aligned} \tag{4}$$

p means prior combination of the time histories. Figure 3a shows the case of the two as-recorded signals presented in Figure 1. The third and fourth graphs show *pGM* and *pVC* respectively. The acceleration responses of the 5% damped SDOF system with a period of 0.17 s are combined in the same way in Figure 3b. In these figures, the maximum values, now called *mpGM* and *mpVC*, are also displayed. In the cases of *pGM* and *pVC*, *GM* and *VC* are displayed (blue squared markers) in the time histories.

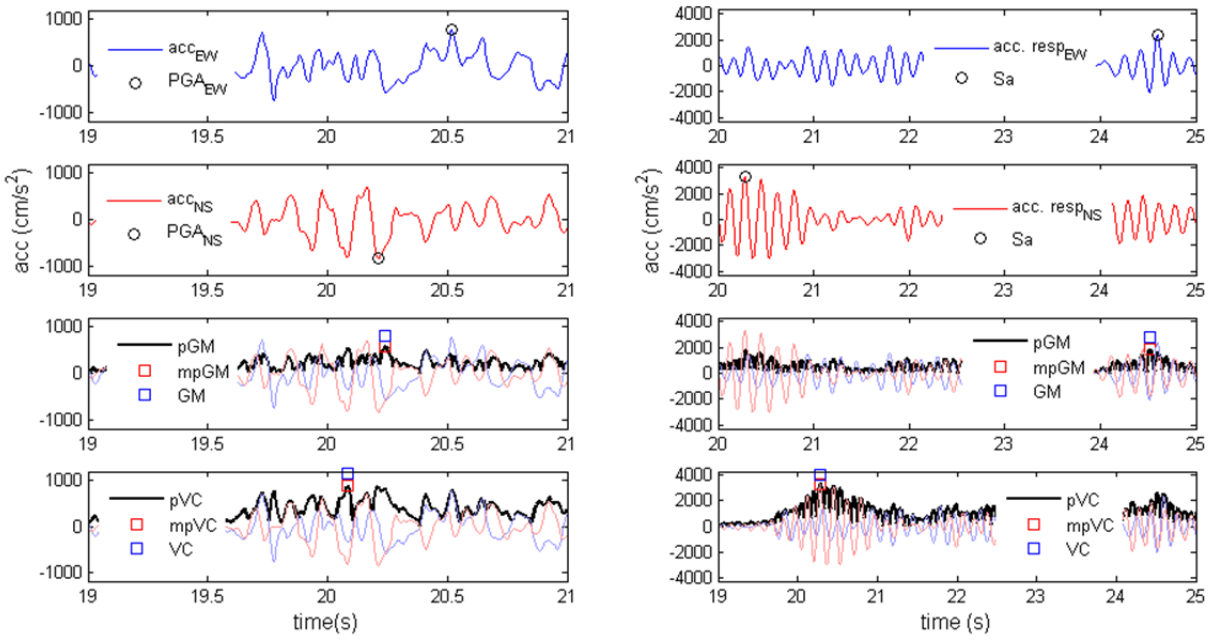

Figure 3. *a) As-recorded accelerograms, pGM and pVC compositions; maximum values, PGA, mpGM and mpVC are marked. GM and VC are also shown. b) Same as a) but for the acceleration responses of a 5% damped SDOF system with a period of 0.17 s.*

Now the two as-recorded signals are rotated, and the maximum values described above are computed. These four peak values, *mpGM*, *mpVC*, *GM*, and *VC*, are shown in Figure 4 as functions of the rotation angle. Because of the symmetry of the rotated components, only the θ-range between 0 and 90º is shown. It can be observed how *mpVC* is θ-invariant; *GM* and *VC* are greater than *mpGM* and *mpVC* respectively. However, *GM* has been widely used to develop strong ground motion predictive equations [Douglas, 2017] in PSHA, because less dispersion is obtained and, of course, they may lead to good average estimates. However, it is important to consider that, in deterministic studies, both *GM* and *VC* have little physical sense. Hence, the new quantities *mpGM* and *mpVC* will be analysed in this study.

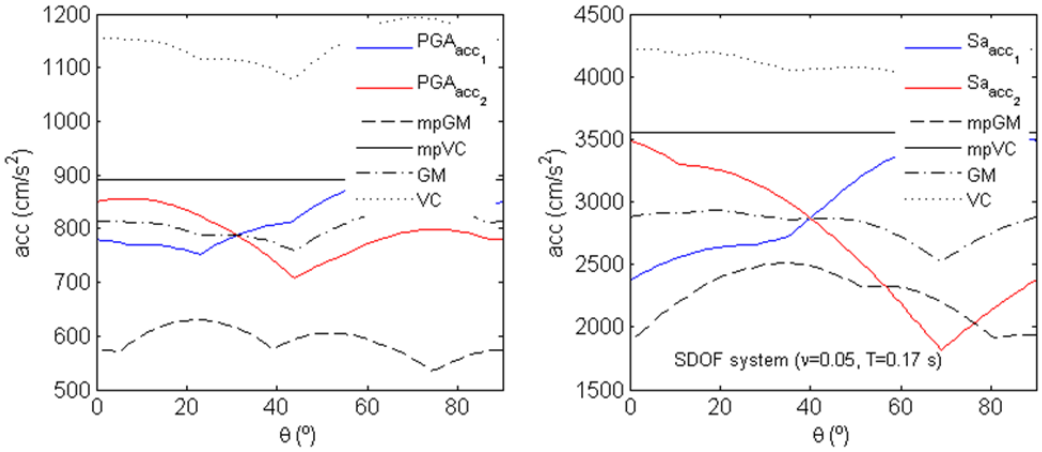

Figure 4. *a) mpGM, mpVC, GM, and VC as functions of the rotation angle, θ, for the as-recorded rotated signals. b) Same as a) for the acceleration responses of the as-recorded rotated signals (ξ=0.05, T=0.17 s).*

3.3 Rotation dependent (RotD) and independent (RotI)

To introduce rotation-dependent (RotD) and rotation-independent (RotI) IMs, Figure 5 shows the response spectra of the as-recorded-rotated signals for angles in the range 0–90º. In this case, a range between 0 and 90º was used as an example. Normally, these two measures are defined with a span of 180º using one of the linear combination $acc_1(t,\theta,T,\xi)$ or $acc_2(t,\theta,T,\xi)$ (see Equation 3). Rotated acceleration time histories, $acc_1(t,\theta,T,\xi)$ and $acc_2(t,\theta,T,\xi)$, are obtained for $\xi = 0.05$ and periods in the range 0.01–1 s, according to Equation (3), and the corresponding response spectra $Sa_{acc1}(T,\theta)$ and $Sa_{acc2}(T,\theta)$ are computed. For each period, T, response spectra values are sorted. Then, the 50th percentile spectrum is obtained, together with the angles at which the 50th percentile spectrum values are attained. Figure 5a shows the response spectra $Sa_{acc1}(T,\theta)$ and $Sa_{acc2}(T,\theta)$. The 50th percentile response spectra are also shown. Figure 5b plots the response spectra as functions of the period and of the rotation angle; the angles at which the 50th percentile values are achieved are also shown.

This kind of spectra are called RotDpp. Rot means rotated, D means dependent on the period, and pp means percentile, which is the 50th in this case. Boore *et al*. [2006] and Boore [2010] proposed the following penalty function that allows us to find the individual response spectrum closest to RotDpp.

$$Penalty(\theta) = \frac{1}{Nper}\sum_{i=1}^{h}\left[\frac{Sa(T_i,\xi,\theta)}{Sa_{RotDpp}(T_i,\xi)} - 1\right]^2 \tag{5}$$

Recall that, in this equation, ξ is the fraction of critical damping. Then, SaRotIpp, is the response spectrum, $Sa(T,\xi,\theta_k)$, and θ_k is the angle that minimizes the *Penalty* function. Note that I means period-independent. Equation (5) has been applied to the response spectra of Figure 5a and Figure 5b, using RotD50 as a target spectrum. The obtained SaRotI50 spectra (green colour lines) are also plotted. The θ_k values are 45º and 48º for acc_1 and acc_2 cases respectively. This technique can be used to find RotDpp and RotIpp for any IM coming from rotated time histories or from their combinations.

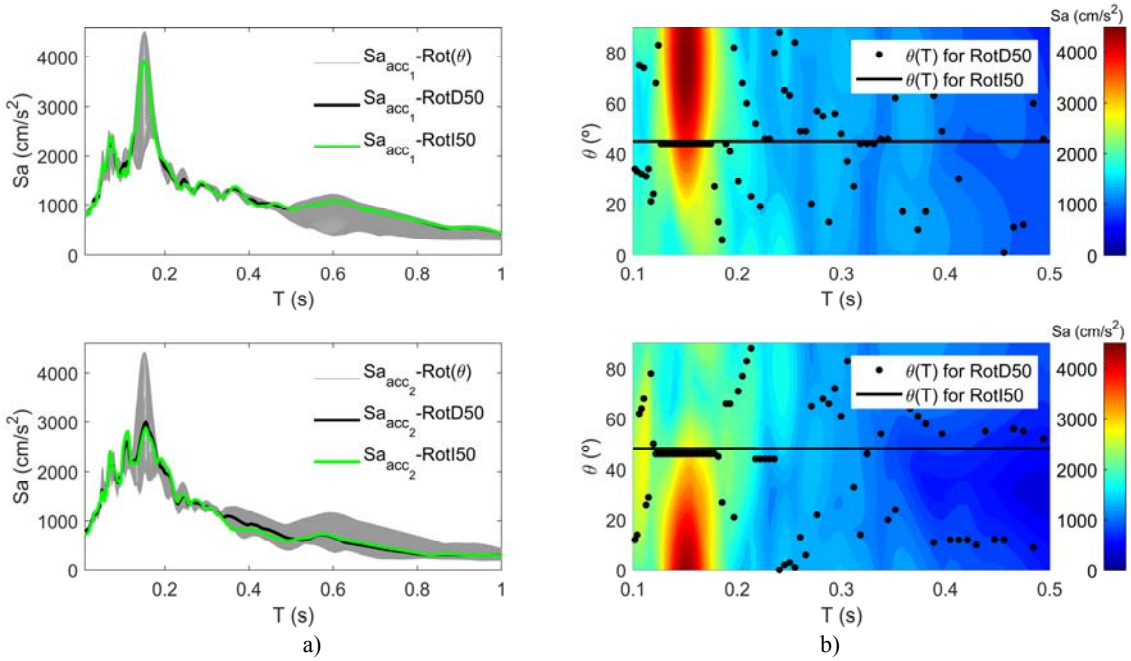

Figure 5. *a) 5% damped response spectra of the rotated accelerograms according to Equation (3);the RotD50 and the RotI50 are also plotted in these figures b)Response spectra as functions of the period, T, and of the rotation angle, θ; the angles θ(T) at which the RotD50 (black dots) and the RotI50 (black line) are achieved are also plotted.*

3.4 Main IMs

PGA and $Sa(T,\xi)$ are the main intensity measures used in PSHA, design, and assessments. The concern originates when a single measure is needed that comes from mixing up IMs corresponding to two orthogonal components. The main IMs used in PSHA are well-described in Douglas [2003]. Two important ways of combining these measures are the GM and the VC, as described above. Thus, in Figure 4, the *mpGM*, *mpVC*, *GM*, and *VC* are shown for the as-recorded rotated accelerograms and for their responses in a SDOF system with ξ=0.05 and T=0.17 s. *GM* is greater than *mpGM* and *VC* is greater than *mpVC*. The physical meaning of *GM* and *VC* is uncertain because of the non-simultaneity of the composed

quantities, although *GM* is used in PSHA as a good statistical estimator of the expected IMs. Note that the *mpVC* is θ-invariant. In fact, *mpVC* is equal to the *resultant*, which is defined in Douglas [2003] as a_r, according to the second line of the following equation.

$$\begin{aligned} mpVC(\theta) &= \max\left[acc_1^2(t,\theta) + acc_2^2(t,\theta) \right]^{1/2}_{\text{for } t} = \\ = \quad a_r &= \max\left[\max\left| acc_1(t,0)\cos\theta + acc_2(t,0)\cos\theta \right|_{\text{for } t} \right]_{\text{for } \theta} \end{aligned} \tag{6}$$

Table 2 summarizes the main IMs used to deal with directionality effects (see also Douglas, 2003). The first column of this table gives the names of the IMs, the second column provides a brief description, and the third column contains a summary of the computation method. RotDpp and RotIpp can be used for any of the IMs in the table. Thus, GMRotD50 and GMRotI50 were used by Boore *et al.* [2006], RotD50 and RotD100 were introduced by Boore [2010], and they are the 50th and 100th percentiles of the response spectra of the two horizontal orthogonal components rotated onto all non-redundant angles. Concerning the maximum values of the combined time histories, the following IMs are analysed: *mpGM*RotDpp, *mpGM*RotIpp, and *mpVC*. The *mpVC(θ)*, that is, the *Resultant* as defined in Douglas [2003] (see also Equation (6), was also identified as the maximum response by Hidalgo *et al*. [2017]. *mpGM*RotD50 and *mpGM*RotI50 correspond to the 50th percentile, period-dependent and period-independent respectively, of the *mpGM(T,ξ,θ)* computed for all non-redundant θ-angles. The *Larger* (also called *Largest* by Douglas, 2003) has been used in several directionality studies [Beyer and Bommer, 2006, Bradley and Baker, 2015, Boore and Kishida, 2016]. This measure was one of the most frequently used in the development of GMPEs before it was realised that the use of geometric mean-based IMs leads to better results in the regressions used in the GMPE calculations. To reduce the epistemic uncertainty of this IM, *LRotD50* and *LRotD100* sensor orientation-independent IMs are proposed. L means Larger in this IMs.

3.5 IMs comparison

The accelerograms recorded at station T1213 on 30 October 2016 in the Central Italy, *Mw*=6.5, Umbria earthquake, have been used to illustrate these important IMs. Figure 6a shows the response spectra of the as-recorded signals for the *mpVC*, *Larger*, *mpGM*, and *GM*. Figure 6b shows a narrower band of periods. This figure also includes the Sa_{NS} and Sa_{EW} acceleration spectra. *NS* is higher than *EW* for almost all the periods. Note that, *Larger* is practically the same as *NS*. Clearly, *m*pVC shows the maximum value in each period followed by *Larger*. The comparison of *mpGM* and *GM* confirms that *GM* is conservative (see also Figure 4). Independent-orientation IMs were evaluated and compared with those obtained by combining the as-recorded accelerograms. In Figure 7, the following three distinct groups of IMs can be seen: i) *mpGM*, *mpGMRotD50*, and *mpGMRotI50* corresponding to the maximum values of the combination of time histories (black), ii) *GM*, *GMRotD50*, and *GMRotI50* corresponding to maximum values of the time histories (red), and iii) *Larger*, *LRotD50*, and *LRotD100* (blue). In this case, *mpGM*, *mpGMRotD50*, and *mpGMRotI50* are similar. Also similar are *GM*, *GMRotD50* and *GMRotI50*, and *RotD50*. Finally, *Larger* and *LRotD50* are very close. *mpVC* has the same values as *RotD100* for every period. However, *LRotD100*, presented in this paper, also has the same values, which indicates a new way to obtain the maximum spectral response.

Table 2. *Summary of the main ground-motion IMs. The name, description and computation method are in the first, second, and third columns respectively.*

Individual time histories		
$acc(t,\theta,T,\xi)$	Absolute acceleration response time history. θ is the axes-rotation-angle. As-recorded accelerograms, acc_1 and acc_2 correspond to $T = 0$ and $\theta = 0$.	Solving equation of motion [Nigam and Jennings, 1969]
$\mathrm{Rot}(T,\xi,\theta)$	Maximum value of $acc(t,\theta,T,\xi)$, for t. $T = 0$ and $\theta = 0$ corresponds to PGA.	$\max(\lvert acc(t,T,\xi,\theta)\rvert)_{\text{for } t}$
Combined two orthogonal time histories		
$pGM(t,T,\xi,\theta)$	Prior combination of the time histories through the geometric mean.	$\lvert acc_1(t,T,\xi,\theta)\ acc_2(t,T,\xi,\theta)\rvert^{1/2}$
$pVC(t,T,\xi,\theta)$	Prior combination of the time histories through vector composition.	$\left[acc_1^2(t,T,\xi,\theta)+acc_2^2(t,T,\xi,\theta)\right]^{1/2}$
$mpGM(T,\xi,\theta)$	Maximum value of $pGM(t,T,\xi,\theta)$ for t	$\max\left[pGM(t,T,\xi,\theta)\right]_{\text{for } t}$
$mpVC(T,\xi,\theta)$	Maximum value of $pVC(t,T,\xi,\theta)$ for t	$\max\left[pVC(t,T,\xi,\theta)\right]_{\text{for } t}$
$GM(T,\xi,\theta)$	Geometric mean of two $Sa(T,\xi,\theta)$ corresponding to two orthogonal time histories. Used in GMPE and in PSHA.	$\left[Sa_1(T,\xi,\theta)\ Sa_2(T,\xi,\theta)\right]^{1/2}$
VC	Vector composition of two $Sa(T,\xi,\theta)$ corresponding to two orthogonal time histories (rarely used).	$\left[Sa_1^2(T,\xi,\theta)+Sa_2^2(T,\xi,\theta)\right]^{1/2}$
$\mathrm{Larger}(T,\xi,\theta)$	Maximum value of the maximum values, for t, of the two time histories. Also called *Largest* (see for instance, Douglas, 2003).	$\max\begin{bmatrix}\max(acc_1(t,T,\xi,\theta))_{\text{for } t}\\ \max(acc_2(t,T,\xi,\theta))_{\text{for } t}\end{bmatrix}$
Time histories resulting from rotating two orthogonal components		
$\mathrm{RotDpp}(T,\xi,\theta)$ (*)	pp percentile of the IMs of the combined θ-rotated time histories. Values at different periods may correspond to different θ-rotated $Sa(T,\xi,\theta)$.	Standard percentile computation methods
$\mathrm{RotIpp}(T,\xi,\theta_{\min})$ (*)	$Sa(T,\xi,\theta_{\min})$ that minimizes the Penalty function of Equation (5), for θ.	Minimizing the Penalty function for θ. (See Equation 5).

(*) $\mathrm{RotDpp}(T,\xi,\theta)$ and $\mathrm{RotIpp}(T,\xi,\theta_{\min})$ can be used for any of the individual and combined IMs

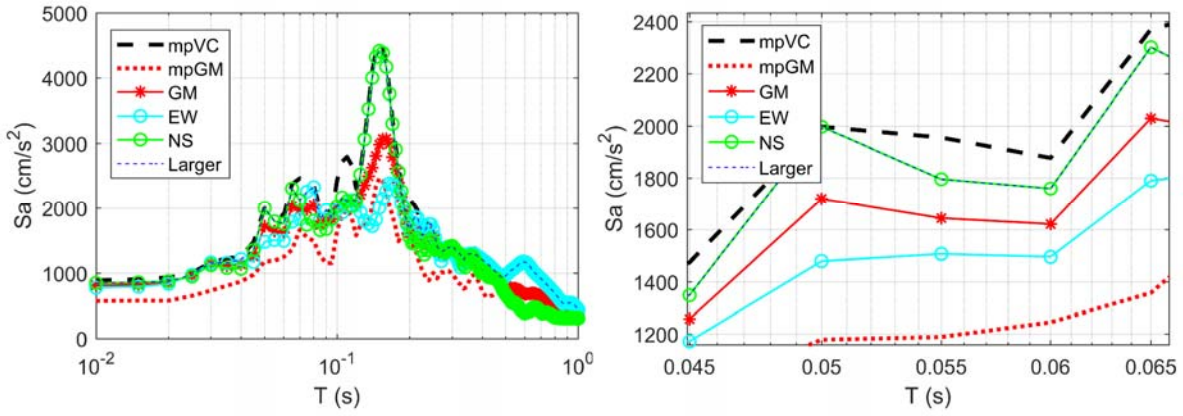

Figure 6. *a) 5% damped response spectra calculated with mpVC, Larger, mpGM, GM, NS, and EW as-recorded IMs from the Umbria earthquake and b) zoom-in range of periods [0.045 0.065]s. This earthquake corresponds to the Central Italy, Mw=6.5, Umbria earthquake, recorded at station T1213, which occurred on 30 October 2016 at 06:40:18.*

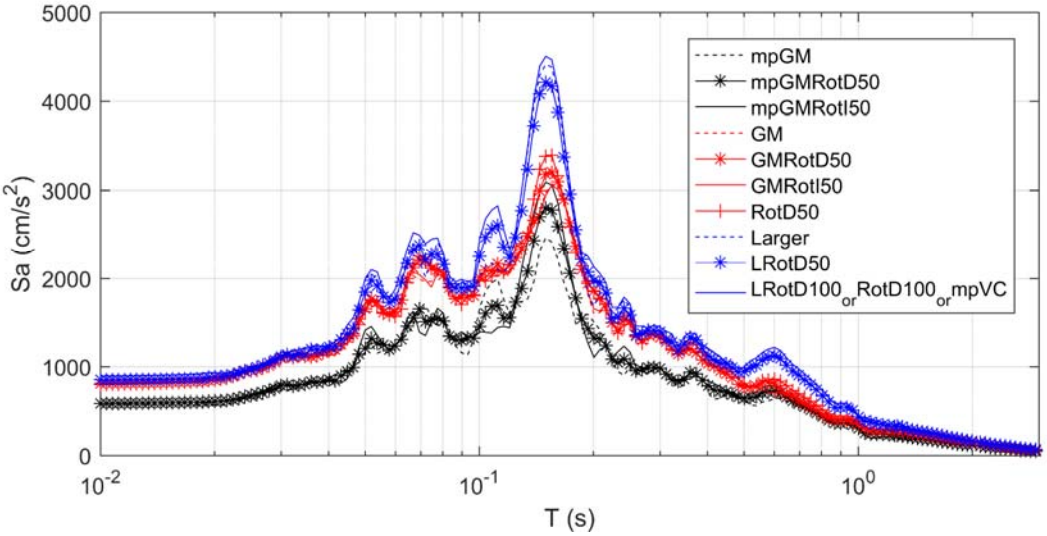

Figure 7. *Comparison among several IMs for the 5% damped response spectra. Note that LRotD100, RotD100, and mpVC are equivalent IMs.*

4 Directionality in Italy

A principal aim of this study is to dimension the impact of the directionality effects on the strong ground motion predictive equations, which have usually been obtained without considering directionality effects. To this end, the geometric mean of the response spectra of the as-recorded acceleration time histories, that is $GM(T,\xi,\theta)$ for θ=0º and ξ=0.05 in Table 2, will be used as a reference because this is the main IM used in PSHA and in GMPE. Ratios between directionality-affected IMs and this reference IM will provide factors, such as functions of the period, indicating the influence of directionality effects and how close to or far from the reference IM are the directionality-affected IMs. As this study is performed for a wide, comprehensive database of strong ground motions in Italy, the results will also be useful for considering, in an easy and straightforward way, the directionality effects in existing PSHA and GMPE in Italy.

The directionality-affected IMs analysed herein are: *SaGMRotD50*, *SaGMRotI50*, and *SaRotD50*. For definitions of the IMs *GM*, *RotDpp*, *RotIpp*, *GMRotDpp*, and *GMRotIpp*, see the explanations in Table 2. *Sa* before these quantities means that 5% damped acceleration response spectra are considered. In addition, ratios for *SaLarger*, *SaLRotD50*, and *SaLRotD100* will be investigated. Note that *SaLRotD100* and *SaRotD100* are equivalent IMs. Moreover, other IMs computed after combining the time histories will be studied too, namely: *SampVC, SampGM*, *SampGMRotD50*, and *SampGMRotI50*. Recall that *RotDpp* measures are period-dependent in the sense that the pp percentile for each period is attained for different rotation angles. In contrast, RotIpp measures are period-independent in the sense that RotIpp correspond to the same rotation angle for all the periods (see Figure 5).

4.1 Data

The database used for this research consists of accelerograms from earthquakes that occurred and were recorded in Italy between 1974 and 2017. This database was collected and standardized first using the records of the Italian Accelerometric Archive [ITACA, Luzi *et al.*,

2016a]. Then, records of events after 31 December 2015 were downloaded from the Engineering Strong-Motion Database [ESM, Luzi *et al*., 2016b]. The complete database has 1583 three-component acceleration records, which correspond to 405 stations and 222 earthquakes. For each record, information about the event (for example, the magnitude, location, and fault mechanism) and about the accelerometric station (epicentral distance, site condition, and location) is available in the header of each file.

The processed accelerograms (corrected data) were used to estimate the response spectra and to obtain the IMs described above. A rigorous selection procedure was applied to the strong ground motion recordings. The following criteria were applied for the selection: depth ($h \leq 30$ km), moment magnitude ($Mw \geq 4$), and epicentral distance ($\Delta \leq 50$ km). After the screening, 949 records corresponding to 249 stations and 131 earthquakes (Figure 8) were available.

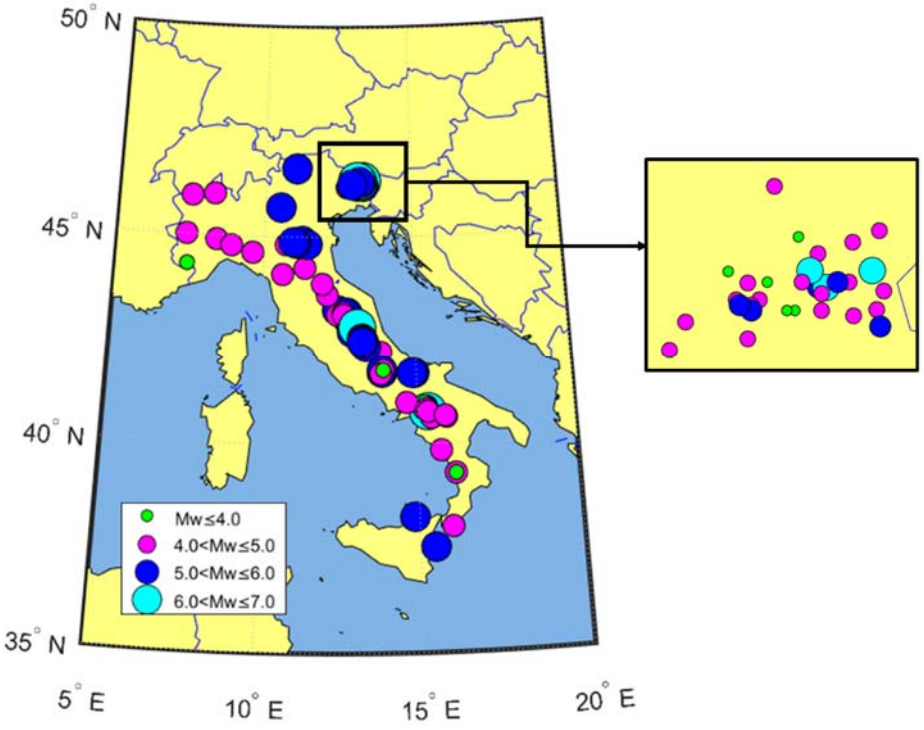

Figure 8. *Epicenters and magnitudes of the earthquakes used in this study.*

4.2 Results

To compare the IMs, we used a MATLAB© script developed by Pinzón [2014] to perform a massive calculation of the two horizontal orthogonal components of the 949 selected records. First, the 5% damped acceleration response spectra were obtained for all the as-recorded signals and for all the linear combinations considered with the rotation angle variation (range 1°–180° with increments of 1°) (see Equation 3). Subsequently, the methods described in Section 3.3 were used to obtain sensor orientation-independent measures. Finally, three groups of ratios were computed. *mpGM*/*GM*, *mpGMRotD50*/*GM*, and *pmGMRotI50*/*GM* are the first group of ratios analysed. Note that *Sa* before these names has been removed for simplicity in the notation. As pointed out above, ratios were computed with GM=$SaGM(T, \xi = 0.05, \theta = 0)$ as the divisor. *GM* was chosen because this is the most common IM used in

PSHA and in GMPE. The second group of ratios is: *GMRotD50*/*GM*, *GMRotI50*/*GM*, and *RotD50*/*GM* and, the third group is *Larger*/*GM*, *LRotD50*/*GM*, and *mpVC*/*GM*. All these quantities are functions of the period in the range 0.01–4 s. Note that most of the records supply information on the range of all the periods. However, the period range is lower for the analogic recordings. Mean values and 95% confidence intervals have been computed for these 9 ratios. For the calculation of the mean values, the antilogarithm of the average of the natural logarithms of the ratios was used, thus representing the GM of the ratios [Shahi and Baker, 2014].

Figure 9a illustrates the first group of ratios. As pointed out above, *GM* is conservative when compared with *mpGM*. Moreover, *mpGMRotD50/GM* and *mpGM/GM* are in the ranges 0.78–0.82 and 0.76–0.80 respectively, which again indicates that *GM* is conservative. Because of the nature of RotD and RotI, both are close to each other. The second group of ratios is shown in Figure 9b. Ratios are close to 1% for *GMRotD50* and they are in the range of 1.5–4.5% for *RotD50*. Again, because of the nature of *GMRotI50*, in this case, ratios are similar to those of *GMRotD50* but a little greater, in the range of 1–2%. The differences increase with increasing periods. These three ratios show good agreement with the results of similar studies in other regions [Boore *et al*., 2006, Boore, 2010, Shahi and Baker, 2014, Bradley and Baker, 2015]. Finally, Figure 9c displays the third group of ratios. For *Larger*, the ratio varies between 14% and 20%. Similar results were reported by Bradley and Baker [2015]. For *LRotD50*, the ratio is in the range of 15–22%, and varies about 1% compared to Larger. No previous information is available on *LRotD50*. We confirm that the maximum value of the vector compositions, *mpVC*, of the two orthogonal components is angle- and period-independent. Our results also confirm that *mpVC* is equal to *RotD100* and *LRotD100*. In this case, the ratios are in the range of 23–31%.

Moreover, the *mpVC*/*GMRotI50* was computed, because this ratio has been evaluated in other studies, namely Beyer and Bommer [2006], BSSC [2009], Campbell and Bozorgnia [2007], Huang *et al*. [2011], and Watson-Lamprey and Boore [2007]. Figure 10 compares our results and those obtained by these authors. They are in good agreement. The first part of the curve is flat around a value of 1.20 and increases to 1.32 at the 4.0 s period. Finally, the influence of magnitude on this last ratio was also investigated. The database was disaggregated into the following magnitude intervals: $4 \leq M_w < 5$, $5 \leq M_w < 6$, and $M_w \geq 6$. An interesting result was obtained: the ratios *mpVC*/*GMRotI50* are in the ranges of 1.24–1.30, 1.20–1.27, and 1.17–1.25 respectively for low, mid and high magnitudes. In the three cases, these ratios increase with increasing periods and differences are greater for low periods. Dispersion is greater for low magnitude events (Figure 11).

Finally, the ratio *mpVC/GMRotI50* was also investigated for two ranges of epicentral distances (Epi); namely, Epi < 15 km and Epi in the range 30–50 km. For this analysis, the events were also separated, according to great ($M_w > 5.5$) and small ($M_w \leq 5.5$) magnitudes. Recall that these two groups of events are known as Type 1 and Type 2 earthquakes in Eurocode-8 (EC-8, CEN, 2004). The range of investigated periods was [0.01 4] s. Figure 12 shows the results. Distance influences the directionality effects. Ratios are greater for short distance earthquakes. Ratios are in the following ranges: 18–37 %, 17–32%, 23–35% and 20–29% respectively for Type 1 near and distant events and Type 2 near and distant events, respectively.

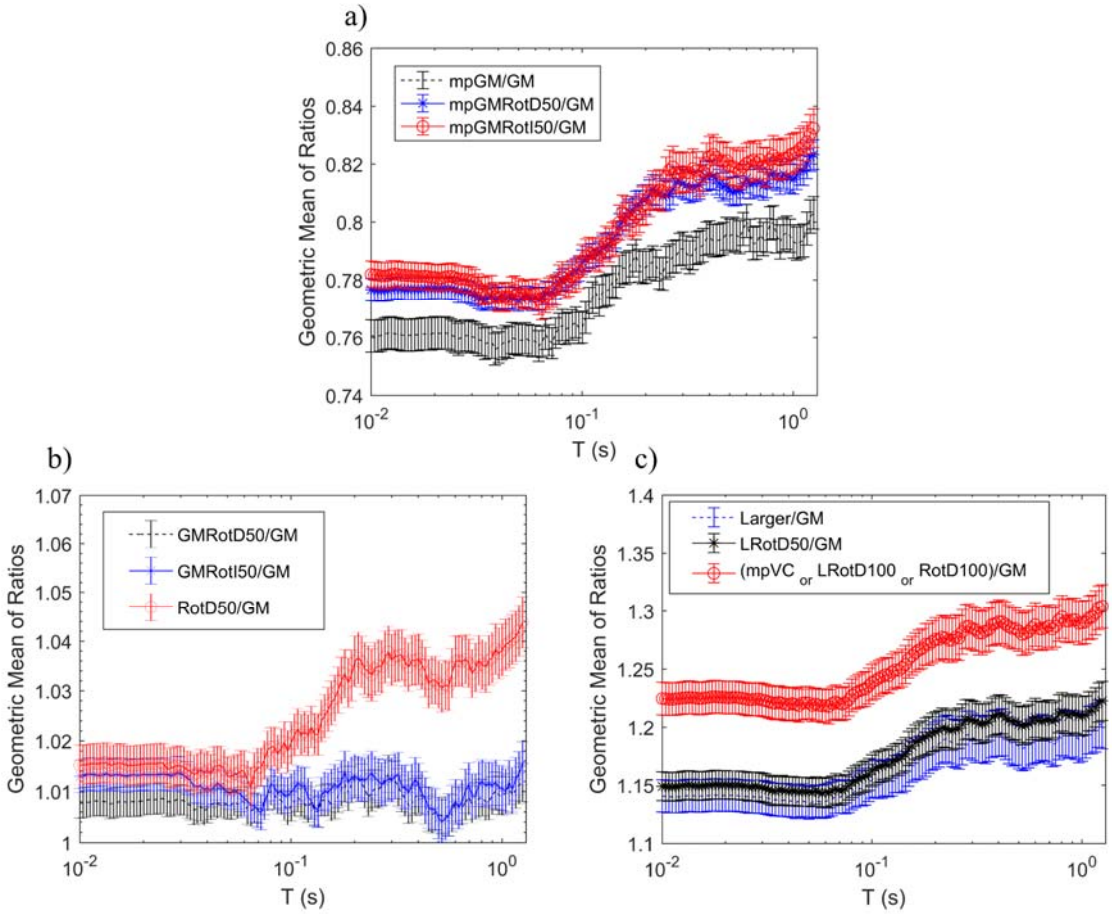

Figure 9. *Ratios for IMs. a) mpGM/GM, mpGMRotD50/GM, and pmGMRotI50/GM; b) GMRotD50/GM, GMRotI50/GM, and RotD50/GM;* c) *Larger*/*GM*, *LRotD50*/*GM*, and *mpVC*/*GM*. *The 95% confidence intervals are also shown.*

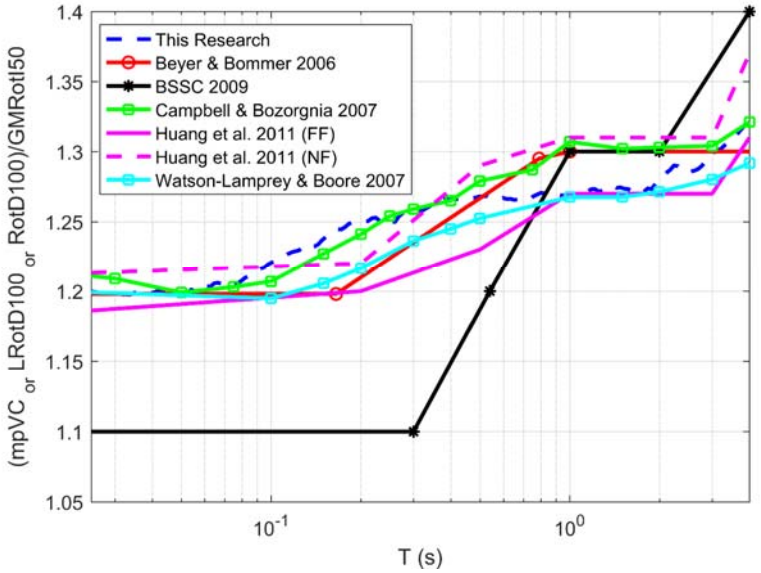

Figure 10. *Geometric mean value of the ratio mpVC/GMRotI50 found in this study and comparison with ratios obtained by others.*

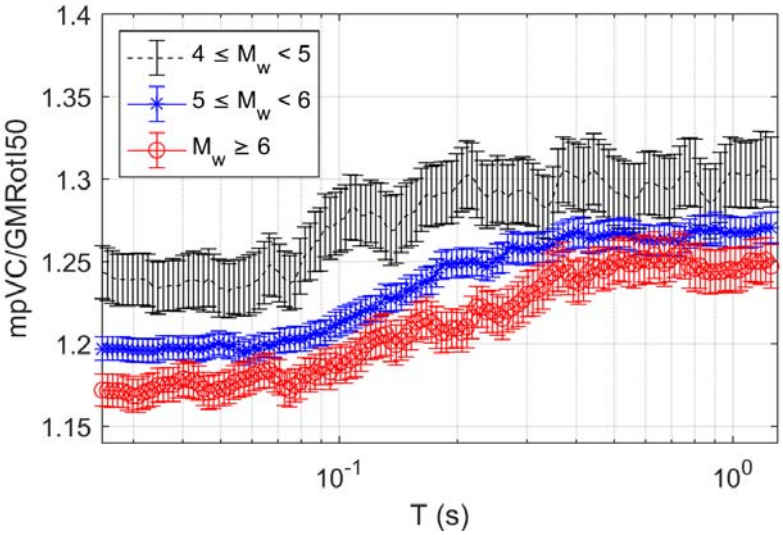

Figure 11. *Geometric mean of the ratio mpVC/GMRotI50* and *95% confidence intervals for different magnitude ranges.*

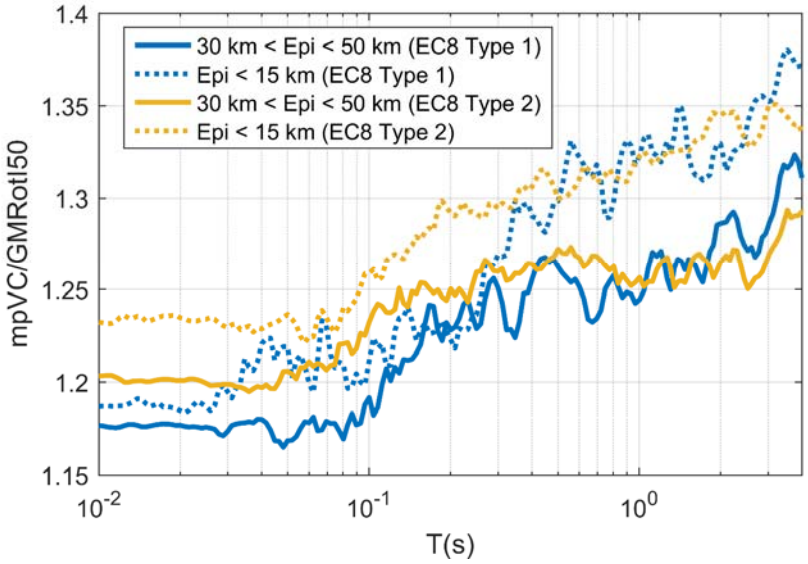

Figure 12. *Geometric mean of the ratio mpVC/GMRotI50 for close and distant, Type 1 and Type 2 events (see the explanation in the text).*

4.3 Model

As can be seen in Figures 9 to 12, the ratios show a typical trend that has been exploited to model the results in a compact way, allowing easy conversion between available IMs that have not considered directionality and Rot-modified IMs. The model is a combination of log-linear functions tuning the obtained ratios. GMRotD50/GM and GMRotI50/GM are very similar, almost constant, in the entire period range (see Figure 9b) and were excluded from this fit. The model is defined as follows:

$$\begin{aligned} \rho = ratio &= Y_1 && \text{for } T<T_1 \\ &= Y_1 + \left(Y_2 - Y_1\right)\left[\frac{\ln\left(T/T_1\right)}{\ln\left(T_2/T_1\right)}\right] && \text{for } T_1 \le T < T_2 \\ &= Y_2 && \text{for } T_2 \le T<T_3 \\ &= Y_2 + \left(Y_3 - Y_2\right)\left[\frac{\ln\left(T/T_3\right)}{\ln\left(T_4/T_3\right)}\right] && \text{for } T_3 \le T \le T_4 \end{aligned} \tag{7}$$

This is a piecewise model that depends on 7 parameters: Y_i(i=1⋯3) and T_j (j=1⋯4). Median values (50 percentiles) have been used in the fit. The model was used to fit the ratios obtained for type 1 and type 2 events [CEN, 2004]. Table 3 shows the number of records for each group. Table 4 and Table 5 show the coefficients of the model of Equation (7) for type 1 and type 2 events, respectively. For comparison purposes, Figure 13 shows the ratio results, which are well-fitted by the model. This model can be used in GMPEs developed in Italy to convert the available IMs to Rot-modified ones.

Table 3. *Ground motions records (NS and EW components) for type 1 and type 2 events.*

EC-8	**Number of records**
Type 1 (M_w> 5.5)	281
Type 2 (M_w≤ 5.5)	668
Total	949

Table 4. *Coefficients for the ratio model for Type 1 earthquakes.*

Ratio	**T1**	**T2**	**T3**	**T4**	**Y1**	**Y2**	**Y3**
RotD50/GM		0.60	2.50		1.01	1.04	1.07
mpGM/GM		0.39	2.00		0.75	0.80	0.83
mpGMRotD50/GM		0.40	2.30		0.77	0.82	0.86
mpGMRotI50/GM	0.10*	0.39	1.72	4.00*	0.77	0.82	0.87
Larger/GM		0.30	2.45		1.13	1.19	1.25
LRotD50/GM		0.40	1.83		1.14	1.21	1.28
mpVC/GM		0.40	2.00		1.21	1.30	1.37

Table 5. *Coefficients for the ratio model for Type 2 earthquakes.*

Ratio	**T1**	**T2**	**T3**	**T4**	**Y1**	**Y2**	**Y3**
RotD50/GM		0.20	0.90		1.02	1.04	1.06
mpGM/GM		0.18	1.00		0.76	0.79	0.82
mpGMRotD50/GM		0.22	1.00		0.78	0.82	0.84
mpGMRotI50/GM	0.07*	0.26	0.90	4.00*	0.78	0.82	0.85
Larger/GM		0.22	1.67		1.14	1.20	1.23
LRotD50/GM		0.22	1.08		1.15	1.21	1.25
mpVC/GM		0.20	1.00		1.23	1.29	1.34

* This value applies to all ratios.

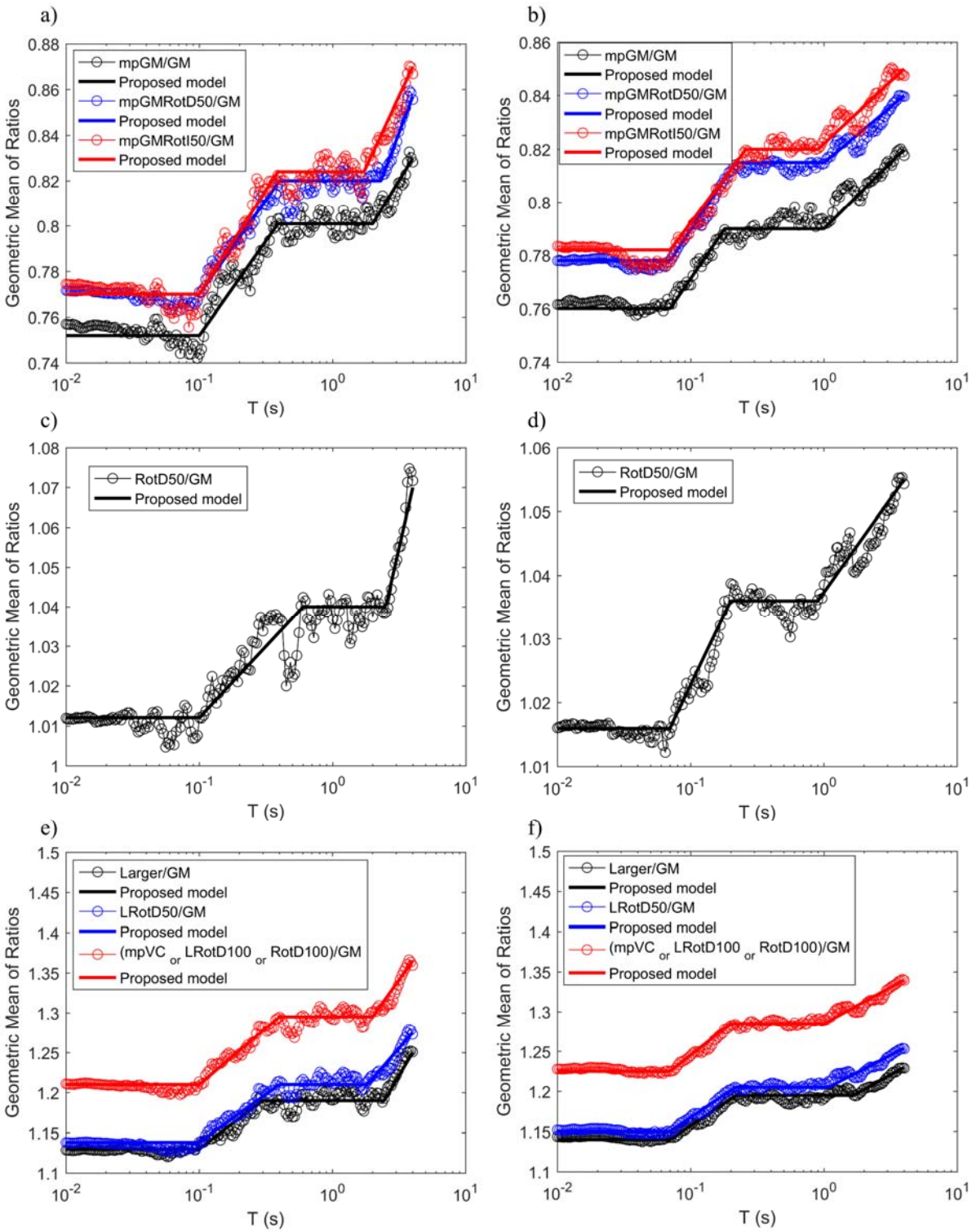

Figure 13. *Sa_{mpGM}/Sa_{GM}, $Sa_{mpGMRotD50}/Sa_{GM}$, and $Sa_{GMRotI50}/Sa_{GM}$ compared to the proposed model for a) EC-8 Type 1 earthquakes; b) EC-8 Type 2 earthquakes. Sa_{RotD50}/Sa_{GM} compared to the proposed model for c) EC-8 Type 1 earthquakes; d) EC-8 Type 2 earthquakes. Ratios Sa_{Larger}/Sa_{GM}, $Sa_{LRotD50}/Sa_{GM}$ and ($Sa_{LRotD100}$ or $Sa_{RotD100}$ or Sa_{mpCV}/Sa_{GM} compared to the proposed model for e) EC-8 Type 1 earthquakes; f) EC-8 Type 2 earthquakes.*

5 Summary, discussion and conclusions

Directionality effects in Italy have been analysed using a large, wide strong ground motion database. As the study involves massive calculations of the responses of 5% critically damped linear SDOF systems, the computing time is considerable. Among other factors, computation time depends on the computer components (hardware), software, and numerical algorithms used in the analysis. In this study, the numerical method proposed by Nigam and Jennings [1969] was implemented. Noticeably, this method produced the same accuracy of results and reduced the computing time around 10 fold compared to the step-by-step numerical integrations of the equation of motion via Duhamel's integral [Pinzón, 2014].

After a discussion and summary of the main IMs involved in directionality analysis, several ratios, related to the most frequently used IMs in PSHA and in GMPE, were debated, computed, and analysed. The main IM used in GMPE is the geometric mean of the peak values [Sa(T)] of the two acceleration response time histories, which, for simplicity, has been called GM here. This IM is conservative in comparison to what is known as *mpGM*, that is, the maximum value of the geometric mean of the time histories.

Special attention has been devoted to the ratio *mpVC/GMRotI50*, and the results are in good agreement with previous directionality studies in other regions. Data have been disaggregated for magnitudes and distances. Directionality effects are more important for low magnitude ($4 \leq M_w < 5.5$) near (dist<15 km) events. Ratios increase with increasing periods. However, differences among ratios are greater for short periods, and smaller for long periods. Finally, to provide an easy tool to incorporate directionality effects in Italy in existing GMPE, a four-linear model was used to fit most of the ratios obtained.

A theoretical advantage of orientation-independent IMs is that they eliminate the sensor orientation effect as a contributor to the epistemic uncertainty. In addition, they are sensor orientation-independent, *GMRotD50*, *GMRotI50*, and *RotD50* IMs are generally larger than the as-recorded GM. Notably, both GMRotI50 and RotD50 have been used by the Pacific Earthquake Engineering Research Center (PEER) NGA GMPEs as new IMs. Similar results to those of Boore *et al*. [2006] and Boore [2010] were obtained. Although the difference between GMRotD50, GMRotI50, RotD50, and GM is small, orientation-independent measures should be used as they decrease epistemic uncertainty in the GMPEs [Beyer and Bommer, 2006].

In this paper, the vector composition of the time histories, *mpVC*, was analysed. It was found that *mpVC* is identical to RotD100 and LRotD100. The *mpVC*/*GMRotI50* ratios obtained are very similar to those calculated in the studies cited above. For all cases, except for the expression proposed by the NEHRP [BSSC, 2009], the *mpVC/GMRotI50* ratio is constant in low periods, with an approximate value of 1.20, increasing until 1.32 in the long period range. In fact, *mpVC*, *RotD100*, and *LRotD100* can be considered the maximum response, corresponding to the most unfavourable case. Consequently, these values could be useful for the design or risk assessment of structures of special importance such as historical-cultural heritage buildings [Casapulla *et al*., 2017] or other high-risk constructions [Wu *et al*., 2017], since they are the maximum values for the available database.

Overall, the results obtained in this study are of significant interest in the improvement of the GMPEs in PSHA and in seismic design and risk assessments. In this respect, a simple theoretical model has been developed. This directionality model for Italy can be used to

improve existing GMPE as it allows us to include directionality effects, by means of simple ratios, into equations obtained without any consideration of directionality.

6 Acknowledgements

This research was partially funded by the Spanish Government's Ministry of Economy and Competitiveness (MINECO) and by the European Regional Development Fund (ERDF) of the European Union (EU) through the project referenced as CGL2015-65913-P (MINECO/ERDF, EU). The first author is supported by a Ph.D. scholarship grant from the Institute for the Training and Development of Human Resources (IFARHU) and the Government of Panama's National Secretariat of Science, Technology, and Innovation (SENACYT).

References

Beyer K., Bommer J.J. (2006). Relationships between median values and between aleatory variabilities for different definitions of the horizontal component of motion. Bulletin of the Seismological Society of America. **96** (4A):1512–1522.

Bommer J.J., Abrahamson N.A., Strasser F.O., *et al*. (2004). The Challenge of Defining Upper Bounds on Earthquake Ground Motions. Seism. Res. Lett **75**(1):82–95.

Boore D.M., Watson-Lamprey J., Abrahamson N.A. (2006). Orientation-independent measures of ground motion. Bulletin of the Seismological Society of America. **96**(4A):1502–1511.

Boore D.M. (2010). Orientation-Independent, Non-geometric-Mean Measures of Seismic Intensity from Two Horizontal Components of Motion. Bulletin of the Seismological Society of America. **100**(4):1830–1835.

Boore D.M., Kishida T. (2016). Relations between Some Horizontal-Component Ground-Motion Intensity Measures Used in Practice. Bulletin of the Seismological Society of America. **107**(1):1–10.

Bradley B.A., Baker J.W. (2015). Ground motion directionality in the 2010-2011 Canterbury earthquakes. Earthquake Engineering & Structural Dynamics. **44**:371–384.

BSSC. (2009). NEHRP Recommended Seismic Provisions for New Buildings and Other Structures. Washington, D.C.

Campbell K.W. and Bozorgnia Y. (2007). Campbell-Bozorgnia NGA Ground Motion Relations for the Geometric Mean Horizontal Component of Peak and Spectral Ground Motion Parameters.

Casapulla C., Maione A., Argiento L. (2017) Seismic analysis of an existing masonry building according to the multi-level approach of the Italian guidelines on cultural heritage. Ingegneria Sismica. **34**(1):40-59.

CEN (Comité Européen de Normalisation) (2004). Eurocode 8: design of structures for earthquake resistance – Part1: general rules, seismic actions and rules for buildings, Comité Européen de Normalisation Brussels, May, http://www.cen.eu/cenorm/homepage.htm.

Chopra A.K. (2017). Dynamics of Structures: Theory and Applications to Earthquake Engineering, 5th Edition, Pearson Prentice Hall.

Douglas J. (2003). Earthquake ground motion estimation using strong-motion records: a review of equations for the estimation of peak ground acceleration and response spectral ordinates. Earth-Science. Rev. **61**(12):43–104.

Douglas J. (2017). Ground motion prediction equations 1964-2016. University of Strathclyde, Glasgow, UK.

Hidalgo-Leiva D.A., Pujades L.G., Díaz S.A. *et al*. (2017). Orientation-independent Measures of Ground Motion for a Database of Central America. 16th World Conference on Earthquake Engineering (16WCEE), Santiago, Chile, 12 pp.

Huang Y., Whittaker A. and Luco N. (2011). Establishing maximum spectral demand for performance-based earthquake engineering: collaborative research with the University of Buffalo and the USGS, Reston, Virginia.

Ingv (2016) Gruppo di Lavoro INGV sul terremoto in centro Italia (2016). Summary report on the October 30, 2016 earthquake in central Italy Mw 6.5, doi: 10.5281/zenodo.16623.

Luzi L., Pacor F., Puglia R. (2016a). Italian Accelerometric Archive v 2.1. Istituto Nazionale di Geofisica e Vulcanologia, Dipartimento della Protezione Civile Nazionale.

Luzi L., Puglia R., Russo E. and ORFEUS WG5 (2016b). Engineering Strong Motion Database, version 1.0. Istituto Nazionale di Geofisica e Vulcanologia, Observatories & Research Facilities for European Seismology.

Nigam N.C., Jennings P.C. (1969). Calculation of Response Spectra From Strong-Motion Earthquake Records. Bull Seismol Soc Am. **59**:909–922.

Pacor F. Paolucci R, Ameri G., Massa M and R. Puglia (2011) Italian strong motion records in ITACA: overview and record processing. Bull Earthquake Eng. **9**:1741–1759. DOI 10.1007/s10518-011-9295-x

Paolucci, R., F. Pacor, R. Puglia, G. Ameri, C. Cauzzi, and M. Massa (2011). Record processing in ITACA, the new Italian strong-motion database, in Earthquake Data in Engineering Seismology: Predictive Models, Data Management, and Networks.Akkar, Sinan, Polat Gülkan, and Torild Van Eck (Editors), Springer, Dordrecht, the Netherlands. Pp 99-113.

Pinzón L.A. (2014). Evaluación de medidas de intensidad del movimiento del suelo independientes de la orientación del sensor para una base de datos con acelerogramas de Costa Rica, El Salvador y Nicaragua. Universitat Politècnica de Catalunya. Retrieved from http://upcommons.upc.edu/pfc/handle/2099.1/24352

Pinzón L.A., Pujades L.G., Diaz S.A., Alva R.E. (2018). Do Directionality Effects Influence Expected Damage? A Case Study of the 2017 Central Mexico Earthquake. Bulletin of the Seismological Society of America. (Published online: August 7, 2018).

Shahi S.K., Baker J.W. (2014). NGA-West2 models for ground-motion directionality. PEER 2013/10. Pacific Earhquake Engineering Research Center, Berkeley, California. 73 pp.

Spudich B.P., Chiou B.S.J., Graves R., *et al.* (2004). A Formulation of Directivity for Earthquake Sources Using Isochrone Theory. U.S. Geol. Surv. Open-File Rept. 2004-1268, 54 pp.

Watson-Lamprey J.A. and Boore D.M. (2007). Beyond SaGMRotI: Conversion to SaArb, SaSN, and SaMaxRot. Bulletin of the Seismological Society of America. **97**:1511–24.

Wu Y., Yan X., Qi A. (2017). Deformation, damage, and collapse of phyllite tunnels under strong earthquake dynamic actions. Ingegneria Sismica. **34**(2):31-48.

ingegneria sismica
International Journal of Earthquake Engineering
Anno XXXV – Num. 3

MODELLI DI DIREZIONALITA' DERIVANTI DA TERREMOTI ITALIANI

Luis A. Pinzón[1], Luis G. Pujades[1], Diego A. Hidalgo-Leiva[2] and Sergio A. Díaz[3]

[1]Department of Civil and Environmental Engineering, Technical University of Catalonia, Barcelona, Spain

[2]Civil Engineering School, University of Costa Rica, San Jose, Costa Rica

[3]Academic Division of Engineering and Architecture, Universidad Juárez Autónoma de Tabasco, Tabasco, Mexico

SUMMARY: *Nel presente lavoro vengono investigati gli effetti della direzione sui sismi violenti attesi in Italia*. Dopo una breve descrizione relativo a tale effetto e alla misura dell'intensità utilizzata, viene utilizzato un vasto database italiano per un totale di 949 accelerogrammi (in due direzioni). Le analisi sono condotte utilizzando spettri di rsiposta con uno smorzamento del 5% nel range di periodi 0.01-4 secondi. Viene investigata una intensità di misura non dipendente dalla direzione che si ottiene combinando i massimi valori degli accelerogrammi considerati. I rapporti tra queste misure di intensità indipendenti dalla rotazione e quelle precedentemente utilizzate nelle equazioni predittive del moto del suolo sono state calcolate e modellate per mezzo di un semplice modello teorico. Pertanto, i risultati sono utili per aggiornare le precedenti equazioni predittive del moto del terreno in modo semplice e diretto.

KEYWORDS: *directionality, seismic response, intensity measures, orientation-independent, spectral response*

.

Corresponding author: Luis A. Pinzón, Department of Civil and Environmental Engineering, Technical University of Catalonia, Spain.
Email: luis.pinzon@upc.edu